

Article

The Mechanism of PEDOT: PSS Films with Organic Additives

Shui-Yang Lien ^{1,2,3}, Po-Chen Lin ⁴, Wen-Ray Chen ⁵, Chuan-Hsi Liu ^{6,*}, Kuan-Wei Lee ⁷ , Na-Fu Wang ⁸
and Chien-Jung Huang ^{4,*}

¹ School of Opto-Electronic and Communication Engineering, Xiamen University of Technology, Xiamen 361024, China

² Department of Materials Science and Engineering, Da-Yeh University, Dacun, Changhua 51591, Taiwan

³ Fujian Key Laboratory of Optoelectronic Technology and Devices, Xiamen University of Technology, Xiamen 361024, China

⁴ Department of Applied Physics, National University of Kaohsiung, Kaohsiung University Rd., Kaohsiung 81148, Taiwan

⁵ Department of Electronic Engineering, National Formosa University, Wenhua Rd., Yunlin 632301, Taiwan

⁶ Department of Mechatronic Engineering, National Taiwan Normal University, Heping East Rd., Taipei 10610, Taiwan

⁷ Department of Electronic Engineering, I-Shou University, No.1, Sec. 1, Syuecheng Rd., Dashu District, Kaohsiung 84001, Taiwan

⁸ Department of Electronic Engineering, Center for Environmental Toxin and Emerging-Contaminant Research, Super Micro Mass Research & Technology Center, Cheng Shiu University, Chengcing Rd., Niasong Dist., Kaohsiung 82146, Taiwan

* Correspondence: liuch@ntnu.edu.tw (C.-H.L.); chien@nuk.edu.tw (C.-J.H.)

Abstract: This article demonstrates changes in the structures of poly (3,4-ethylene dioxythiophene): polystyrene sulfonate (PEDOT: PSS) with the addition of organic additives. The mechanisms of PEDOT: PSS are analyzed using X-ray photoelectron spectroscopy (XPS), cross-sectional images obtained from scanning electron microscopy (SEM), and contact angles. In this paper, a bond-breaking reaction and phase separation are successfully found to occur between PEDOT: PSS molecules and the organic additives. Our research also finds that this bond-breaking reaction and phase separation exist in the PEDOT: PSS–sorbitol–maltitol film at the same time. The addition of organic additives will improve the optical properties and the moisture stability of PEDOT: PSS films.

Keywords: PEDOT: PSS; organic additive; bond-breaking reaction; phase separation



Citation: Lien, S.-Y.; Lin, P.-C.; Chen, W.-R.; Liu, C.-H.; Lee, K.-W.; Wang, N.-F.; Huang, C.-J. The Mechanism of PEDOT: PSS Films with Organic Additives. *Crystals* **2022**, *12*, 1109. <https://doi.org/10.3390/cryst12081109>

Academic Editor:
Younes Hanifehpour

Received: 14 July 2022
Accepted: 4 August 2022
Published: 8 August 2022

Publisher's Note: MDPI stays neutral with regard to jurisdictional claims in published maps and institutional affiliations.



Copyright: © 2022 by the authors. Licensee MDPI, Basel, Switzerland. This article is an open access article distributed under the terms and conditions of the Creative Commons Attribution (CC BY) license (<https://creativecommons.org/licenses/by/4.0/>).

1. Introduction

Since optoelectronic devices became popular, more and more teams have been studying them. It is worth noting that indium tin oxide (ITO) is the most common material used for optoelectronics applications due to its low conductivity and high transparency. However, ITO as a material also has some disadvantages, such as a shortage on Earth and requirements such as a high temperature and a vacuum process for fabrication. Hence, more and more studies have tried to find a low-cost material to replace ITO. To respond to this need, conductive polymer material [1–5], carbon-based nanomaterials [6–8], metallic nanostructures [9–11], and multilayer thin films [12–14] have been explored as transparent electrodes. Among them, the high polymer material poly (3,4-ethylenedioxythiophene): polystyrene-sulfonate (PEDOT: PSS) is a better option owing to its advantages such as high transparency, low haze, and large-area application for its commercial availability. Currently, an increasing number of researchers regard PEDOT: PSS as a potential material for replacing indium tin oxide (ITO) in industrial applications.

However, PEDOT: PSS has a fatal flaw: its low conductivity of about 1090 S/cm, but after the addition of organic additives to PEDOT: PSS, the conductivity will increase. In 2002, Kim et al. discovered that organic additives such as dimethyl sulfoxide, *N,N*-dimethyl formamide, and tetrahydrofuran can be added to PEDOT: PSS [15]. Their research determined

that the shielding effect between PEDOT and PSS is due to polar additives and pointed out the importance of temperature and σ_{DC} for charge transport properties. After that, a rising number of teams researched the addition of polar organic additives (DMSO, EG, DMF, sorbitol, maltitol, and xylitol) into a PEDOT: PSS solution to improve conductivity [16–19]. It was found that the structure of PEDOT: PSS changes after doping with organic additive. These phenomena can be used to enhance the conductivity of PEDOT: PSS films. Some polar additives can achieve phase separation between PEDOT: PSS and can form an ordered PEDOT layer under the PSS layer, which can enhance the charge migration rate. Our team pointed out that the PEDOT: PSS doped with organic additives will achieve a bond-breaking reaction and phase separation [20]. Adding sorbitol to PEDOT: PSS can achieve a bond-breaking reaction, which can increase the transparency of the film [21]. Adding maltitol to PEDOT: PSS can achieve phase separation due to the screening effect, which can change the structure of the film [20]. The team of Liangqi Ouyang also found that additives, such as dimethyl sulfoxide, ethylene glycol, and Polyethylene glycol 400, induced a separation between PSS and PEDOT in highly conductive PEDOT: PSS films [22]. In another study, quantum dots, acid treatment, and heat treatment were used to change the structure of PEDOT: PSS films. Fei-Peng Du et al. constructed PEDOT: PSS composite films with graphene quantum dots to enhance the thermoelectric performance of the film, which increased the electrical conductivity to 7172 S/m [23]. These apparent improvements were attributed to the ordered arrangement of PEDOT chains on the surface of graphene. There is a strong interfacial interaction between PEDOT: PSS and graphene and a separation of the PEDOT and PSS phases. Acid treatments and annealing can both reorganize the structure of the film. Mengistie et al. exploited formic acid to treat PEDOT: PSS layers to then obtain a high-transparency and high-electrical-conductivity film [24]. After the formic acid treatment, the conductivity of the PEDOT: PSS film increased to 2050 S/m. The enhanced conductivity in the PEDOT: PSS layer was due to the high dielectric constant of the formic acid, which could induce a shielding effect between the PEDOT and the PSS. From the research of Qi Geng et al., it was also found that phase separation occurred during the heat treatment of a PEDOT: PSS solution. It allowed the dispersed PEDOT to agglomerate into strips and to form a conductive grid [25]. They also found that the conductivity of the PEDOT: PSS film after annealing increased to 1305 S/cm.

In this study, adding 4 wt.% sorbitol to PEDOT: PSS can cause a bond-breaking reaction, and adding 4 wt.% maltitol to PEDOT: PSS can cause phase separation. Moreover, mixing sorbitol and maltitol at a ratio of 1:1 in PEDOT: PSS can be used to determine that a bond-breaking reaction and phase separation occur at the same time. Additionally, a detailed investigation of the bond-breaking reaction and phase separation is presented.

2. Materials and Methods

2.1. Material

The PEDOT: PSS was purchased from Heraeus (1.3–1.7 wt.% from H. C. Starck Baytron P AI-4083, purchased from Heraeus Co., Hanau, Germany), maltitol was procured from Alfa Aesar (Alfa Aesar, Shanghai, China, $C_{12}H_{24}O_{11}$, 97%), sorbitol was obtained from Sigma (St. Louis, MO, USA, $C_6H_{14}O_6$, 98%), and formic acid was secured from Sigma (St. Louis, MO, USA, CH_2O_2 , 98%).

2.2. Experimental Details

The glass was cut into 3 cm \times 3 cm as glass substrates. The substrates were cleaned with acetone, methanol, and deionized water in an ultra-sonicator for 10 min. After that, the substrate was surface passivated for 120 s using oxygen plasma at 20 W. The sorbitol (4 wt.%) was added to PEDOT: PSS (hereinafter referenced as PEDOT: PSS–sorbitol), and the maltitol (4 wt.%) was added to PEDOT: PSS (hereinafter referenced as PEDOT: PSS–maltitol), and the mixture of sorbitol and maltitol at a ratio of 1:1 was added to PEDOT: PSS (hereinafter referenced as PEDOT: PSS–sorbitol–maltitol). The reason we utilized the concentration of 4 wt.% is because of its upper solubility limit. All of the mixtures were

stirred with a stirrer at 300 rpm and baked at 100 °C for 20 min on a hot plate. The precursor was coated onto the substrate with a spin-coating process utilizing a spinner at the first stage at 500 rpm for 10 s and at the second stage at 2000 rpm for 20 s. Adding a low coating stage can ensure evenness of the film, which is a nanomaterial [26]. Subsequently, the film was baked at 100 °C for 20 min.

2.3. Characteristic Measurements

The surface morphology of the film was observed by scanning electron microscopy (SEM; 6330TF, JEOL, Taipei, Taiwan). The film was quantified by X-ray photoelectron spectroscopy (XPS; PHI 5000, ULVAC-PHI, Hagisono, Chigasaki, Kanagawa Prefecture, Japan).

3. Results

3.1. XPS Spectra of PEDOT: PSS with and without Organic Additives

The surface chemical elements and structures of PEDOT: PSS were characterized by X-ray photoelectron spectroscopy (XPS). Typical carbon spectra (C 1s) of PEDOT: PSS are shown in Figure 1. In Figure 1a, the peak at 284.3 eV is attributed to the C=C chain of α -PEDOT [27]. The peak at 285.1 eV is assigned to the C=C chain of β -PEDOT [27], and the peak at 286.3 eV is attributed to C-O/C-S chains [23]. In Figure 1b, the peak at 285.1 eV is gone, which shows that the β -PEDOT disappeared. This phenomenon is also due to the bond-breaking reaction and disturbs the PEDOT chain, which is induced by sorbitol. In Figure 1b, the peak at 288.1 eV is attributed to the C=O chain [28]. In Figure 1c, it is worth noting that the peak 288.1 eV shifted to 287.3 eV, which is assigned to the C-O-C chain [29]. This phenomenon is due to phase separation, which is induced by maltitol. The addition of maltitol transformed the PEDOT chain from a benzoid structure to a quinoid structure [30]. Additionally, the XPS image of PEDOT: PSS–maltitol shows that the β -PEDOT also disappeared. This leads to the conclusion that the addition of organic additives to PEDOT: PSS removes the peak of β -PEDOT. In Figure 1d, the XPS image displays both a bond-breaking reaction and phase separation, letting the peak of 287.3 eV shift to 287.6 eV and inducing a peak at 288.7 eV.

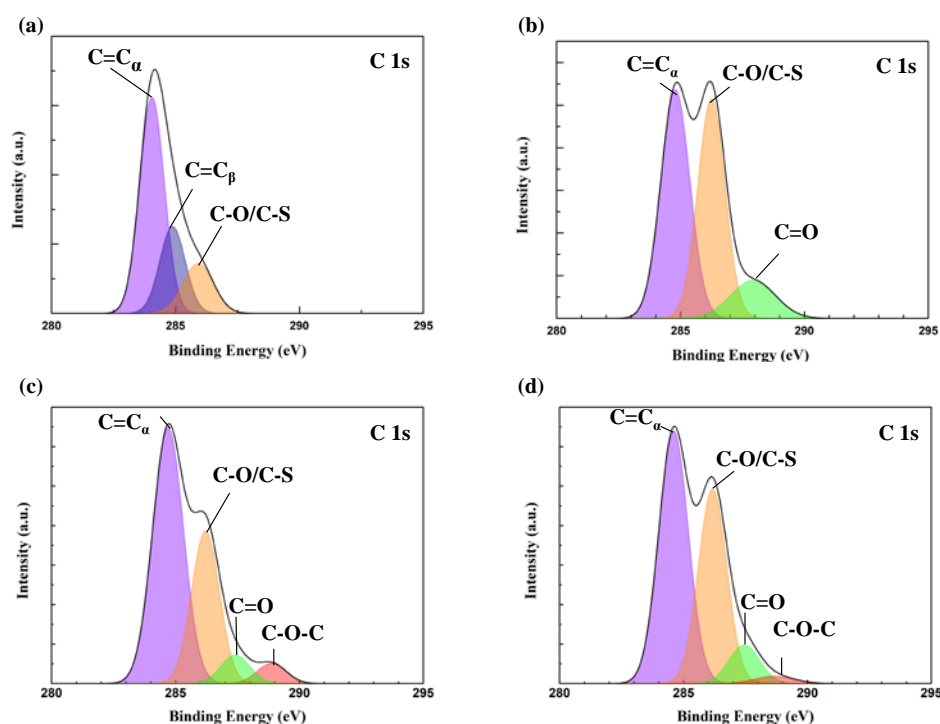


Figure 1. C (1s) peak of XPS spectra for (a) PEDOT: PSS, (b) PEDOT: PSS–sorbitol, (c) PEDOT: PSS–maltitol, and (d) PEDOT: PSS–sorbitol–maltitol.

The XPS spectrum of S 2p peaks is shown in Figure 2. In Figure 2, the peaks at 163.3 eV and 164.7 eV are presented for S 2P_{3/2} and S 2P_{1/2}, which are from the PEDOT. Additionally, the peaks at 167.2 eV and 168.8 eV are presented for the S 2P_{3/2} and S 2P_{1/2} of PSS. For the ratio between PEDOT and PSS, the area is displayed in Table 1. In Table 1, the sample of PEDOT: PSS presents the ratio of PEDOT and PSS as 0.51%. For the sample PEDOT: PSS–sorbitol, the ratio of PEDOT and PSS is 0.69%. This phenomenon is consistent with the suggestion by Jonsson et al. that excess PSS is washed away during the film-forming process [31]. Additionally, it is worth noting that the ratio between PEDOT and PSS for the sample PEDOT: PSS–maltitol is 0.96%. It has a large increase due to the phase separation, which is induced by the maltitol additive. It will cause the film of PEDOT: PSS film to separate so that the PSS layer floats on the surface of the film. Additionally, after the spin-coating process, the PSS layer is thrown out. For the PEDOT: PSS–sorbitol–maltitol sample, the ratio between PEDOT and PSS decreased to 0.72%, which is shown in Table 1. This decline is due to the existence of phase separation and a bond-breaking reaction in the PEDOT: PSS–sorbitol–maltitol film.

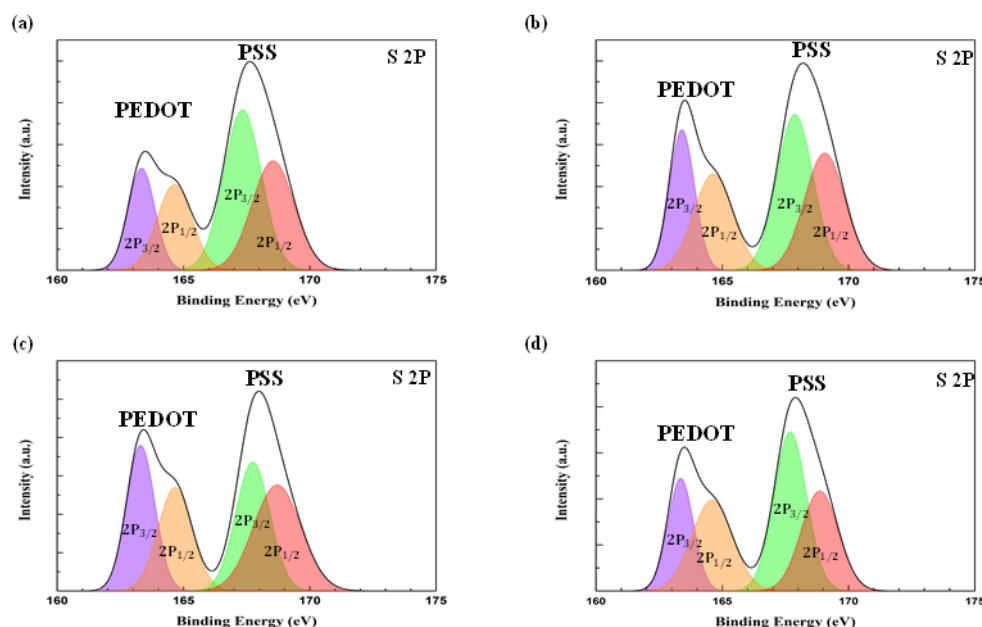


Figure 2. S (2p) peak of XPS spectra for (a) PEDOT: PSS, (b) PEDOT: PSS–sorbitol, (c) PEDOT: PSS–maltitol, and (d) PEDOT: PSS–sorbitol–maltitol.

Table 1. The XPS (S 2p) area ratio of PEDOT: PSS doped with sorbitol and maltitol.

Sample	PEDOT Area Ratio (%)	PSS Area Ratio (%)	Ratio (PEDOT/PSS)
PEDOT: PSS	34	66	0.51
PEDOT: PSS–sorbitol	41	59	0.69
PEDOT: PSS–maltitol	49	51	0.96
PEDOT: PSS–sorbitol–maltitol	42	58	0.72

To further understand the mechanism of PEDOT: PSS with and without organic additives, the XPS sputter in-depth profile was analyzed. In Figure 3a, the C 1s, O 1s, and S 2p of PEDOT: PSS are measured. In Figure 3b, the increasing curve of C 1s is attributed to cross-linkage associated with the C=C double bonds at 12 min [32]. In Figure 3b, the line of O 1s appears before 6 min. This phenomenon has shown that the addition of sorbitol achieved a bond-breaking reaction and produced sulfide ions. In Figure 3c, the increasing curve of C 1s is due to phase separation, which is achieved by the maltitol additive. This indicates that there is a strong interaction with PEDOT chains after phase separation. It is worth noting that the sulfur signals at 7 min are weak, which suggests that the PEDOT

chains were coated with enriched-PSS chains. In Figure 3c, the declining O 1s line at 6 min is due to the phase separation, with PEDOT chains destroying the crystalline region and the stack structure of PEDOT: PSS [23]. In Figure 3d, the XPS sputter in-depth profile of the PEDOT: PSS–sorbitol–maltitol film is similar to Figure 3c. This phenomenon occurred when the film achieved phase separation.

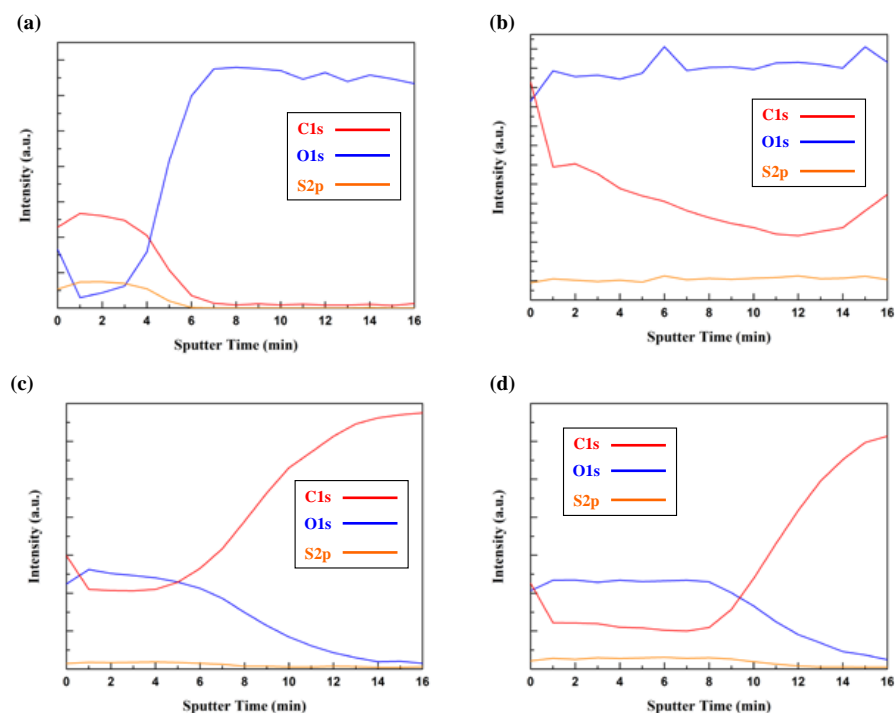


Figure 3. XPS sputter in-depth profile for (a) PEDOT: PSS, (b) PEDOT: PSS–sorbitol, (c) PEDOT: PSS–maltitol, and (d) PEDOT: PSS–sorbitol–maltitol.

3.2. Cross-Sectional SEM Micrograph of Bond-Breaking Reaction and Phase Separation

To further understand the changes in the PEDOT: PSS after phase separation and bond-breaking reactions. Scanning electron microscopy (SEM) cross-sectional images of PEDOT: PSS, PEDOT: PSS with sorbitol, PEDOT: PSS with maltitol, and PEDOT: PSS with sorbitol and maltitol are shown in Figure 4. In Figure 4a, the thickness of PEDOT: PSS is about 497.3 nm, as shown in Table 2. The morphology of the cross-sectional shows that the coil-like PEDOT: PSS curled together. In Figure 5, the schematic of the PEDOT: PSS structure and formation of the film are displayed, which is consistent with the conjecture by the team of Jonathan Rivnay [33]. In Figure 4b, the thickness of PEDOT: PSS–sorbitol declined to 179.5 nm, as shown in Table 2. This phenomenon was confirmed as the result of a purge of PEDOT: PSS during the spin-coating process [32]. In addition, there is a round bump (red circle) on the image, which can be referenced as a PEDOT: PSS particle, as shown in Figure 4b. This can confirm that sorbitol added to PEDOT: PSS achieves a bond-breaking reaction. In Figure 4c, it can be observed that there is a PSS layer floating on the PEDOT layer and that the total thickness is 315.6 nm, as shown in Table 2. The upper layer accounts for the PSS layer (96.1 nm), and the lower layer is considered the PEDOT layer (219.5 nm), which confirms that phase separation is achieved by adding maltitol to PEDOT: PSS. This result is also consistent with the result of Table 1 showing that the upper PSS layer is removed during the spin-coating process. In Figure 4d, the thickness of PEDOT: PSS–sorbitol–maltitol is 184.4 nm, as shown in Table 2. It can be seen that there is a layer floating on the left and that the thickness is 75.3 nm, which is also referred to as the PSS layer. Meanwhile, there is a core–shell particle (red circle) laying on the right site. Both properties confirm that PEDOT: PSS–sorbitol–maltitol can achieve a bond-breaking reaction and phase separation at the same time.

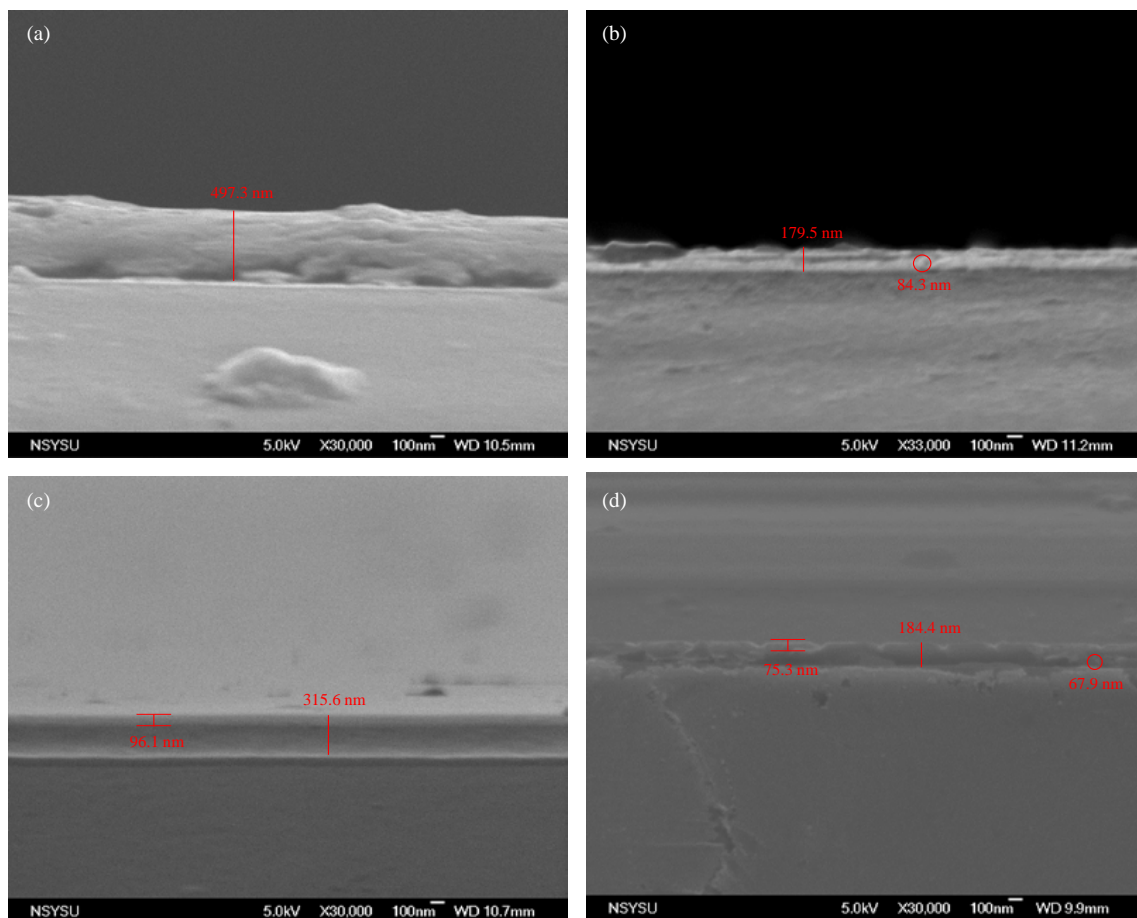


Figure 4. Scanning electron microscopy (SEM) micrograph of the cross sections of (a) PEDOT: PSS, (b) PEDOT: PSS–sorbitol, (c) PEDOT: PSS–maltitol, and (d) PEDOT: PSS–sorbitol–maltitol.

Table 2. The thicknesses of PEDOT: PSS doped with organic additives.

Sample	Thickness (nm)
PEDOT: PSS	497.3
PEDOT: PSS–sorbitol	179.5
PEDOT: PSS–maltitol	315.6
PEDOT: PSS–sorbitol–maltitol	184.4

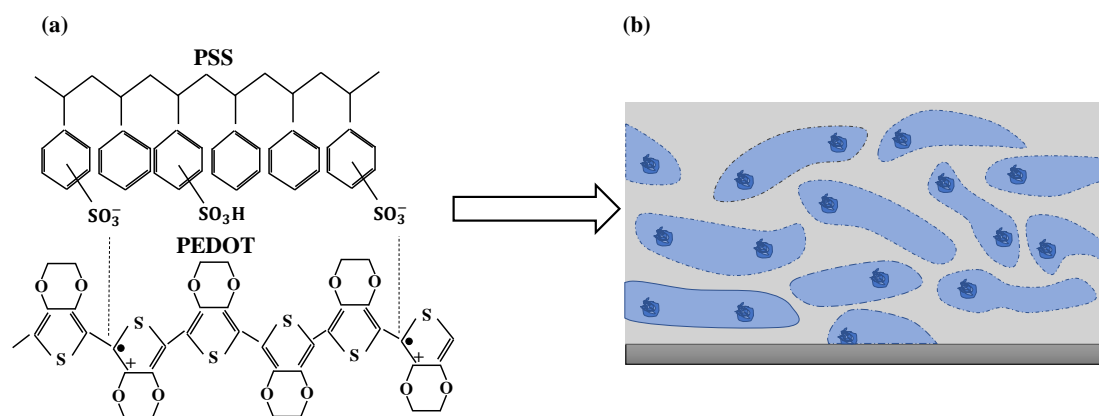


Figure 5. PEDOT: PSS structure and morphology: (a) PEDOT: PSS molecular structure and (b) resultant film with the PEDOT: PSS-rich (blue) and PSS-rich (grey) phases.

3.3. Contact Angle Analysis of PEDOT: PSS Doped with the Organic Additives

Measuring the contact angle can be used to further understand the mechanism behind the addition of organic additives to PEDOT: PSS. In Figure 6a, the contact angle result of the pristine PEDOT: PSS film is 25.7° , which is the contact angle of methane with PEDOT: PSS. Methane is used to measure the contact angle because PEDOT: PSS films are highly hydrophilic. In Figure 6b, the contact angle result of the PEDOT: PSS–sorbitol film is 32.7° . The results show that the addition of sorbitol to PEDOT: PSS causes a change in the PEDOT: PSS structure. In Figure 6c, the contact angle of the PEDOT: PSS–maltitol film increases to 39.5° , which confirms the existence of phase separation. This phenomenon confirms that adding maltitol can achieve phase separation and lets the hydrophobic PSS layer float on the PEDOT layer. This result is additional evidence to confirm the existence of phase separation, which also matches the image in Figure 4c. In Figure 6d, the contact angle of the PEDOT: PSS–sorbitol–maltitol film declines to 35.6° , which is between the contact angles of PEDOT: PSS–sorbitol film and PEDOT: PSS–maltitol film. It can be explained by the PEDOT: PSS–sorbitol–maltitol film exhibiting both phase separation and bond-breaking reaction at the same time. In conclusion, this is breakthrough evidence that can confirm the existence of a bond-breaking reaction and phase separation in PEDOT: PSS–sorbitol–maltitol film at the same time.

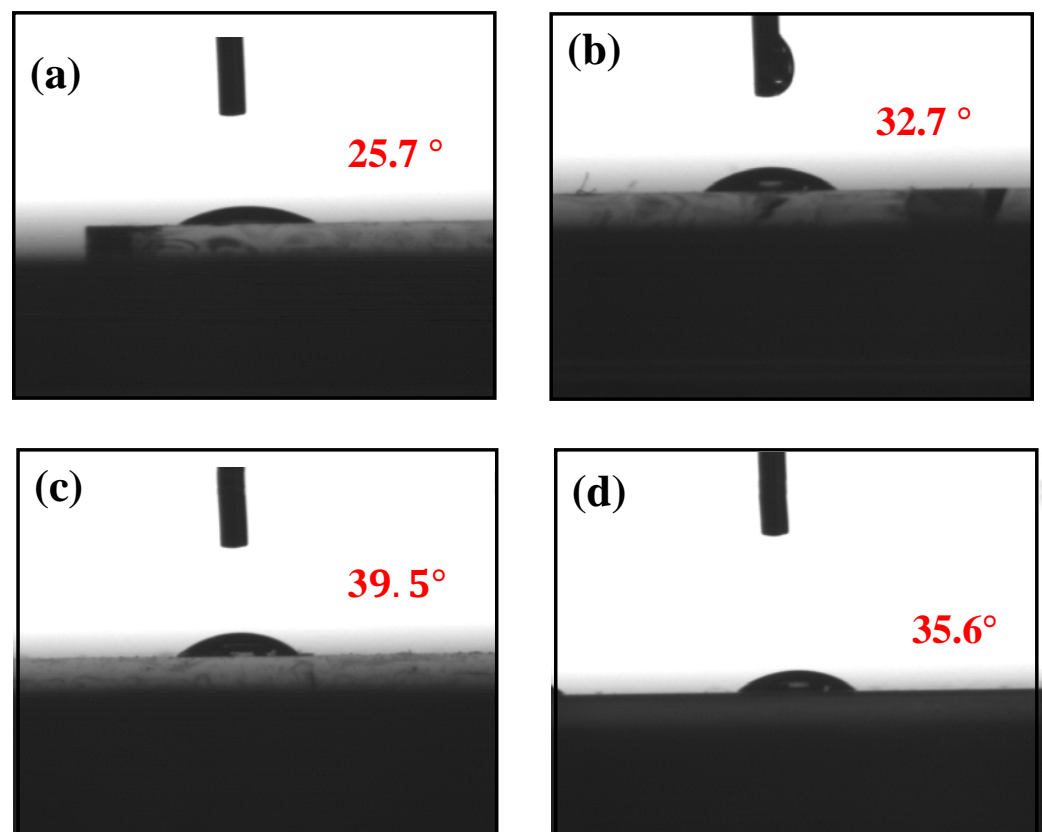


Figure 6. Contact-angle measurements with methane for (a) PEDOT: PSS, (b) PEDOT: PSS–sorbitol, (c) PEDOT: PSS–maltitol, and (d) PEDOT: PSS–sorbitol–maltitol.

4. Conclusions

In summary, the cross-sectional image of PEDOT: PSS–maltitol is clearly layered, with a PSS layer and a PEDOT layer. Various techniques—XPS, SEM, and contact angle—showed the mechanism of PEDOT: PSS with or without organic additives. It can be attributed to the existence of phase separation in the PEDOT: PSS–maltitol film. The cross-sectional image of PEDOT: PSS–sorbitol–maltitol also shows the existence of phase separation and a bond-breaking reaction at the same time. In our study, the mechanism behind the bond-breaking

reaction was investigated. Based on the evidence presented above, different mixtures of organic additives added to PEDOT: PSS can achieve different properties.

Author Contributions: Conceptualization, S.-Y.L., K.-W.L., N.-F.W. and P.-C.L.; formal analysis, S.-Y.L., P.-C.L. and C.-J.H.; funding acquisition, P.-C.L. and S.-Y.L.; investigation, S.-Y.L. and C.-J.H.; resources, P.-C.L.; supervision, W.-R.C., S.-Y.L., C.-H.L., N.-F.W. and C.-J.H.; writing—original draft, P.-C.L. All authors have read and agreed to the published version of the manuscript.

Funding: This research was funded by the Ministry of Science and Technology (MOST) of the Republic of China: grant number 110-2221-E-390-019.

Data Availability Statement: The data presented in this study are available from the corresponding author upon request.

Conflicts of Interest: The authors declare no conflict of interest.

References

1. Namsheer, K.; Rout, C.S. Conducting polymers: A comprehensive review on recent advances in synthesis, properties and applications. *RSC Adv.* **2021**, *11*, 5659–5697.
2. Naskar, P.; Maiti, A.; Chakraborty, P.; Kundu, D.; Biswas, B.; Banerjee, A. Chemical supercapacitors: A review focusing on metallic compounds and conducting polymers. *J. Mater. Chem. A* **2021**, *9*, 1970–2017. [[CrossRef](#)]
3. Maziz, A.; Özgür, E.; Bergaud, C.; Uzun, L. Progress in conducting polymers for biointerfacing and biorecognition applications. *Sens. Actuators Rep.* **2021**, *3*, 100035. [[CrossRef](#)]
4. Luo, H.; Kaneti, Y.V.; Ai, Y.; Wu, Y.; Wei, F.; Fu, J.; Cheng, J.; Jing, C.; Yuliarto, B.; Eguchi, M.; et al. Nanoarchitected porous conducting polymers: From controlled synthesis to advanced applications. *Adv. Mater.* **2021**, *33*, 2007318. [[CrossRef](#)]
5. Terán-Alcocer, Á.; Bravo-Plascencia, F.; Cevallos-Morillo, C.; Palma-Cando, A. Electrochemical sensors based on conducting polymers for the aqueous detection of biologically relevant molecules. *Nanomaterials* **2021**, *11*, 252. [[CrossRef](#)] [[PubMed](#)]
6. Serrano-Aroca, Á.; Takayama, K.; Tuñón-Molina, A.; Seyran, M.; Hassan, S.S.; Pal Choudhury, P.; Uversky, V.N.; Lundstrom, K.; Adadi, P.; Palù, G.; et al. Carbon-based nanomaterials: Promising antiviral agents to combat COVID-19 in the microbial-resistant era. *ACS Nano* **2021**, *15*, 8069–8086. [[CrossRef](#)]
7. Singla, S.; Sharma, S.; Basu, S.; Shetti, N.P.; Aminabhavi, T.M. Photocatalytic water splitting hydrogen production via environmental benign carbon based nanomaterials. *Int. J. Hydrog. Energy* **2021**, *46*, 33696–33717. [[CrossRef](#)]
8. Liu, D.; Gu, W.; Zhou, L.; Wang, L.; Zhang, J.; Liu, Y.; Lei, J. Recent advances in MOF-derived carbon-based nanomaterials for environmental applications in adsorption and catalytic degradation. *Chem. Eng. J.* **2022**, *427*, 131503. [[CrossRef](#)]
9. Zhang, Z.; Liu, G.; Cui, X.; Gong, Y.; Yi, D.; Zhang, Q.; Zhu, C.; Saleem, F.; Chen, B.; Lai, Z.; et al. Evoking ordered vacancies in metallic nanostructures toward a vacated Barlow packing for high-performance hydrogen evolution. *Sci. Adv.* **2021**, *7*, eabd6647. [[CrossRef](#)]
10. Martínez, A.; Apip, C.; Meléndrez, M.F.; Domínguez, M.; Sánchez-Sanhueza, G.; Marzalletti, T.; Catalán, A. Dual antifungal activity against *Candida albicans* of copper metallic nanostructures and hierarchical copper oxide marigold-like nanostructures grown in situ in the culture medium. *J. Appl. Microbiol.* **2021**, *130*, 1883–1892. [[CrossRef](#)]
11. Ahmed, H.B.; Emam, H.E. Overview for multimetallic nanostructures with biomedical, environmental and industrial applications. *J. Mol. Liq.* **2021**, *321*, 114669. [[CrossRef](#)]
12. Ekmekcioglu, M.; Erdogan, N.; Astarlioglu, A.T.; Yigen, S.; Aygun, G.; Ozyuzer, L.; Ozdemir, M. High transparent, low surface resistance ZTO/Ag/ZTO multilayer thin film electrodes on glass and polymer substrates. *Vacuum* **2021**, *187*, 110100. [[CrossRef](#)]
13. Poisson, J.; Polgar, A.M.; Fromel, M.; Pester, C.W.; Hudson, Z.M. Preparation of Patterned and Multilayer Thin Films for Organic Electronics via Oxygen-Tolerant SI-PET-RAFT. *Angew. Chem. Int. Ed.* **2021**, *60*, 19988–19996. [[CrossRef](#)]
14. Pandey, A.; Dalal, S.; Dutta, S.; Dixit, A. Structural characterization of polycrystalline thin films by X-ray diffraction techniques. *J. Mater. Sci. Mater. Electron.* **2021**, *32*, 1341–1368. [[CrossRef](#)]
15. Kim, J.Y.; Jung, J.H.; Lee, D.E.; Joo, J. Enhancement of electrical conductivity of poly (3,4-ethylenedioxythiophene)/poly (4-styrenesulfonate) by a change of solvents. *Synth. Met.* **2002**, *126*, 311–316. [[CrossRef](#)]
16. Ahmad, Z.; Azman, A.W.; Buys, Y.F.; Sarifuddin, N. Mechanisms for doped PEDOT: PSS electrical conductivity improvement. *Mater. Adv.* **2021**, *2*, 7118–7138.
17. Alhashmi Alamer, F.; Badawi, N.M. Manufacturing Organic Environmentally Friendly Electrical Circuits Using the Composites' Single-Walled Carbon Nanotubes and PEDOT: PSS. *Energy Technol.* **2022**, *10*, 2100830. [[CrossRef](#)]
18. Liu, H.; Lee, J.; Kang, J. Improving the Sensitivity of an Organic Photodetector by Adding a Polar Solvent to the Hole-Transport Layer for Indirect X-ray Detection. *J. Nanosci. Nanotechnol.* **2021**, *21*, 2992–2997. [[CrossRef](#)]
19. Chen, Y.; Meng, J.; Xu, Y.; Li, Y.; Zhang, Q.; Hou, C.; Sun, H.; Wang, G.; Wang, H. Integrated Ionic-Additive Assisted Wet-Spinning of Highly Conductive and Stretchable PEDOT: PSS Fiber for Fibrous Organic Electrochemical Transistors. *Adv. Electron. Mater.* **2021**, *7*, 2100231. [[CrossRef](#)]

20. Lien, S.Y.; Lin, P.C.; Chen, W.R.; Liu, C.H.; Sze, P.W.; Wang, N.F.; Huang, C.J. Improving Optoelectrical Properties of PEDOT: PSS by Organic Additive and Acid Treatment. *Crystals* **2022**, *12*, 537. [[CrossRef](#)]
21. Khasim, S.; Pasha, A.; Roy, A.S.; Parveen, A.; Badi, N. Effect of secondary doping using sorbitol on structure and transport properties of PEDOT–PSS thin films. *J. Electron. Mater.* **2017**, *46*, 4439–4447. [[CrossRef](#)]
22. Ouyang, L.; Musumeci, C.; Jafari, M.J.; Ederth, T.; Inganas, O. Imaging the phase separation between PEDOT and polyelectrolytes during processing of highly conductive PEDOT: PSS films. *ACS Appl. Mater. Interfaces* **2015**, *7*, 19764–19773. [[CrossRef](#)] [[PubMed](#)]
23. Du, F.P.; Cao, N.N.; Zhang, Y.F.; Fu, P.; Wu, Y.G.; Lin, Z.D.; Shi, R.; Amini, A.; Cheng, C. PEDOT: PSS/graphene quantum dots films with enhanced thermoelectric properties via strong interfacial interaction and phase separation. *Sci. Rep.* **2018**, *8*, 6441. [[CrossRef](#)] [[PubMed](#)]
24. Mengistie, D.A.; Ibrahim, M.A.; Wang, P.C.; Chu, C.W. Highly conductive PEDOT: PSS treated with formic acid for ITO-free polymer solar cells. *ACS Appl. Mater. Interfaces* **2014**, *6*, 2292–2299. [[CrossRef](#)]
25. Geng, Q.; Wang, Z.; Gao, Z.; Gao, T.; Li, Y.; Chen, L.; Li, M. Phase Separation to Improve the Conductivity and Work Function of the PEDOT: PSS Solution for Silicon Hybrid Solar Cells. *J. Phys. Chem. C* **2021**, *125*, 26379–26388. [[CrossRef](#)]
26. Lang, U.; Müller, E.; Naujoks, N.; Dual, J. Microscopical Investigations of PEDOT:PSS Thin Films. *Adv. Funct. Mater.* **2009**, *19*, 1215–1220. [[CrossRef](#)]
27. Mitraka, E.; Jafari, M.J.; Vagin, M.; Liu, X.; Fahlman, M.; Ederth, T.; Berggren, M.; Jonsson, M.P.; Crispin, X. Oxygen-induced doping on reduced PEDOT. *J. Mater. Chem. A* **2017**, *5*, 4404–4412. [[CrossRef](#)]
28. Han, F.; Dai, S.; Yang, J.; Shen, J.; Liao, M.; Xie, H.; Chen, C. Glycerol phosphate dimethacrylate: An alternative functional phosphate ester monomer to 10-methacryloyloxydecyl dihydrogen phosphate for enamel bonding. *ACS Omega* **2020**, *5*, 24826–24837. [[CrossRef](#)]
29. Boeva, Z.A.; Milakin, K.A.; Pesonen, M.; Ozerin, A.N.; Sergeyev, V.G.; Lindfors, T. Dispersible composites of exfoliated graphite and polyaniline with improved electrochemical behaviour for solid-state chemical sensor applications. *RSC Adv.* **2014**, *4*, 46340–46350. [[CrossRef](#)]
30. Lenz, A.; Kariis, H.; Pohl, A.; Persson, P.; Ojamäe, L. The electronic structure and reflectivity of PEDOT: PSS from density functional theory. *Chem. Phys.* **2011**, *384*, 44–51. [[CrossRef](#)]
31. Jönsson, S.K.M.; Birgerson, J.; Crispin, X.; Greczynski, G.; Osikowicz, W.; Van Der Gon, A.D.; Salaneck, W.R.; Fahlman, M. The effects of solvents on the morphology and sheet resistance in poly (3,4-ethylenedioxythiophene)–polystyrenesulfonic acid (PEDOT–PSS) films. *Synth. Met.* **2003**, *139*, 1–10. [[CrossRef](#)]
32. Wong, K.W.; Yip, H.L.; Luo, Y.; Wong, K.Y.; Lau, W.M.; Low, K.H.; Chow, H.F.; Gao, Z.Q.; Yeung, W.L.; Chang, C.C. Blocking reactions between indium-tin oxide and poly (3,4-ethylene dioxythiophene): Poly (styrene sulphonate) with a self-assembly monolayer. *Appl. Phys. Lett.* **2002**, *80*, 2788–2790. [[CrossRef](#)]
33. Rivnay, J.; Inal, S.; Collins, B.A.; Sessolo, M.; Stavrinidou, E.; Strakosas, X.; Tassone, C.; Delongchamp, D.M.; Malliaras, G.G. Structural control of mixed ionic and electronic transport in conducting polymers. *Nat. Commun.* **2016**, *7*, 11287. [[CrossRef](#)] [[PubMed](#)]